Journal of Alzheimer's Disease 58 (2017) 389–400
DOI 10.3233/JAD-161236
IOS Press

A Multifunctional Biocompatible Drug Candidate is Highly Effective in Delaying Pathological Signs of Alzheimer's Disease in 5XFAD Mice

Hadar Segal-Gavish[a,1], Ortal Danino[b,1], Yael Barhum[a], Tali Ben-Zur[a], Ella Shai[c], David Varon[c], Daniel Offen[a,*] and Bilha Fischer[b,*]
[a]*Laboratory of Neuroscience, Felsenstein Medical Research Center, Sackler Faculty of Medicine, Tel Aviv University, Tel Aviv, Israel*
[b]*Department of Chemistry, Bar-Ilan University, Ramat-Gan, Israel*
[c]*Department of Hematology, Hadassah University Hospital, Jerusalem, Israel*

Accepted 5 March 2017

Abstract.
Background: Metal-ion-chelation was suggested to prevent zinc and copper ions-induced amyloid-β (Aβ) aggregation and oxidative stress, both implicated in the pathophysiology of Alzheimer's disease (AD). In a quest for biocompatible metal-ion chelators potentially useful for AD therapy, we previously tested a series of nucleoside 5'-phosphorothioate derivatives as agents for decomposition of Cu(I)/Cu(II)/Zn(II)-Aβ-aggregates, and as inhibitors of OH radicals formation in Cu(I) or Fe(II)/H_2O_2 solution. Specifically, in our recent study we have identified 2-SMe-ADP(α-S), designated as SAS, as a most promising neuroprotectant.
Objective: To further explore SAS ability to protect the brain from Aβ toxicity both *in vitro* and *in vivo*.
Methods: We evaluated SAS ability to decompose or inhibit the formation of $A\beta_{42}$-M(II) aggregates, and rescue primary neurons and astrocytes from $A\beta_{42}$ toxicity. Furthermore, we aimed at exploring the therapeutic effect of SAS on behavioral and cognitive deficits in the 5XFAD mouse model of AD.
Results: We found that SAS can rescue primary culture of neurons and astrocytes from $A\beta_{42}$ toxicity and to inhibit the formation and dissolve $A\beta_{42}$-Zn(II)/Cu(II) aggregates. Furthermore, we show that SAS treatment can prevent behavioral disinhibition and ameliorate spatial working memory deficits in 5XFAD mice. Notably, the mice were treated at the age of 2 months, before the onset of AD symptoms, for a duration of 2 months, while the effect was demonstrated at the age of 6 months.
Conclusion: Our results indicate that SAS has the potential to delay progression of core pathological characteristics of AD in the 5XFAD mouse model.

Keywords: P2Y receptors, nucleotides, amyloid-β aggregates, metal-ion chelation, neuroprotection, 5XFAD mouse model, behavioral disinhibition, spatial working memory

INTRODUCTION

Amyloid-β (Aβ) peptide is known to form aggregates with zinc and copper ions *in vitro* [1, 2] and in Alzheimer's disease (AD) patients [3]. In addition, dyshomeostasis of zinc and copper have been implicated in oxidative stress-related neurotoxicity

[1]These authors contributed equally to this work.

*Correspondence to: Prof. Bilha Fischer, Department of Chemistry, Bar-Ilan University, Ramat-Gan 52900, Israel. Tel.: +927 3 5318303; E-mail: bilha.fischer@biu.ac.il and Prof. Daniel Offen, Felsenstein Medical Research Center, Rabin Medical Center, Petah Tikva 49100, Israel. E-mail: danioffen@gmail.com.

in AD [4, 5]. Metal-ion-chelation was suggested to prevent both metal-ion-induced Aβ aggregation and oxidative stress [6]. In a quest for biocompatible metal-ion chelators potentially useful for AD therapy, we previously tested a series of nucleoside 5'-phosphorothioate derivatives as biocompatible agents for decomposition of Cu(I)/Cu(II)/Zn(II)-Aβ-aggregates, and as inhibitors of OH radicals formation in Cu(I) or Fe(II) /H_2O_2 solution (Fenton reaction) [2].

For instance, we identified ATP-γ-S-(α,β-CH_2), APCPPγS, as a potent chelator which re-solubilized $A\beta_{40}$-Cu(II) aggregates more efficiently than EDTA. Moreover, APCPPγS rescued primary neurons from $A\beta_{42}$ toxicity (IC_{50} 0.2 μM). Importantly, APCPPγS resisted hydrolysis by ecto-nucleotidases [7]. These findings demonstrated the potential of nucleoside-5'-phosphorothioate analogues in general, and APCPPγS in particular, for AD therapy.

A recent approach suggests that activation of P2Y-receptors (P2Y-Rs) by endogenous extracellular nucleotides can protect neurons from oxidative damage [8–10].

P2Y receptors, which are widely expressed in the nervous system, were suggested to mediate remodeling following trauma, stroke, ischemia, or in neurodegenerative disorders [10, 11]. It was hypothesized that ATP, which is released during brain injury, is correlated with the neuroprotective responses by its interaction with P2Y-Rs, mainly $P2Y_1$-R receptor [13]. $P2Y_1$-R is also stimulated by ATP-γ-S, ADP-β-S, and 2-SMe-ADP, which were also demonstrated to enhance neuroprotection [14].

These reports prompted our search for novel and biocompatible neuroprotectants, acting via purinergic receptors, as well as metal-ion chelation. Specifically, we have demonstrated that 2-SMe-ADP(α-S), designated as SAS (Fig. 1), reduced reactive oxygen species (ROS) production within PC12 cells under oxidizing conditions, IC_{50} 0.08 versus 21 μM for ADP. Furthermore, SAS rescued primary neurons subjected to oxidation, EC_{50} 0.04 versus 19 μM for ADP. SAS is also a most potent $P2Y_1$-R agonist, EC_{50} 0.0026 μM. In addition, SAS is stable in human blood serum, $t_{1/2}$ 15 versus 1.5 h for ADP, and resists hydrolysis by NPP1/3, two-fold more than ADP [15].

The potent neuroprotective activity of SAS encouraged us to further explore its ability to provide protection against Aβ toxicity. Here, we evaluated its ability to decompose or inhibit the formation of $A\beta_{42}$-M(II) aggregates, and rescue primary neurons

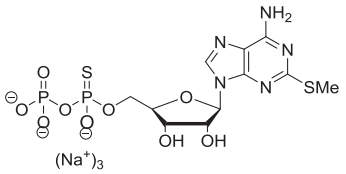

Fig. 1. Chemical structure of SAS.

and astrocytes against $A\beta_{42}$ toxicity. Furthermore, we aimed at exploring the therapeutic effect of SAS on behavioral and cognitive deficits in a mouse model of AD, the 5XFAD model.

The 5XFAD model is a widely-accepted mouse model for AD. This model co-expresses five familial AD mutations of amyloid precursor protein (APP) and Presenilin-1 (PSEN1) that ultimately increase $A\beta_{42}$ generation. 5XFAD mice produce $A\beta_{42}$ almost exclusively and rapidly exhibit robust plaque deposition proportional to cerebral accumulation of $A\beta_{42}$. Amyloid deposition and related gliosis starts at 2 months and reaches a heavy burden mainly in deep cortical layers and subiculum. Prior to plaque formation, 5XFAD mice accumulate intraneuronal $A\beta_{42}$ that aggregates mainly in large pyramidal neurons of the aforementioned brain areas. By 9 months, 5XFAD mice demonstrate marked loss of large pyramidal neurons in cortical layer 5 and subiculum [16].

At 6 months of age, hippocampal synaptic dysfunctions, such as reductions in long-term potentiation at Schaffer collateral-CA1 synapses, emerge in 5XFAD mice. Concomitant with the onset of hippocampal synaptic failures, 5XFAD mice begin to display impairments in hippocampus-dependent memory formation at 6 months of age, as evaluated by the contextual fear conditioning test [17]. Further studies demonstrated that at 4–6 months of age, 5XFAD mice are impaired in spatial memory as evidenced by using the Y-maze alternation test [16] and the Morris water maze task [18]. Additionally, at 9 months of age, 5XFAD mice exhibit anxiety-related behavior in the elevated plus maze assay [19].

MATERIALS AND METHODS

Materials

SAS was prepared according to Azran et al. [15]. DMEM medium, glutamine, and penicillin-streptomycin-nystatin were obtained from Biological Industries, Inc. (Kibbutz Beit Haemek, Israel). $FeSO_4$, $Cu(NO_3)_2$, and ATP were obtained from

Sigma Chemical Co. (St. Louis, MO). Human $A\beta_{42}$ was obtained from GL-Biochem (Shanghai, China).

Turbidity assays

Freeze-dried monomeric $A\beta_{42}$ was prepared according to Amir et al. [2] and dissolved in 50 mM Tris-HCl (pH 7.4) to obtain a 50 μM stock solution. From this solution the following samples of controls and $A\beta_{42}$-Zn(II)/Cu(II) aggregates were prepared by the addition of 50 μM $ZnCl_2$ or $Cu(NO_3)_2$ in H_2O: 1) 50 μM $A\beta_{42}$; 2) 50 μM $A\beta_{42}$-Zn(II)/Cu(II); 3) 50 μM $A\beta_{42}$-Zn(II) and SAS/EDTA (150 μM final concentration); 4) SAS or EDTA at 150 μM were added to 50 μM $A\beta_{42}$-Zn(II)/Cu(II) solution after 1 h. These samples were incubated at 37°C for 4 h to form aggregates. An 80 μL of each of solutions was taken to UV absorbance at 405 nm and measured every hour in triplicate. Tris-HCl buffer was used as the blank.

Preparation of primary neuron cultures

As we previously described, newborn rat brains (one-day-old) were removed under sterile conditions, the cortex was dissected and separated from the remaining brain, roughly homogenized by repeating pippetation, and then trypsinized [20]. The trypsin was removed from the dissociated cells by centrifugation at 4,000 rpm, and dissociated cells were plated at a density of 4 10^5/mL into 96 multi-well plates (Nunc, Naperville, IL) that had been precoated with polyornithine (15 μg/mL). Cells were cultured in a serum-free medium composed of a mixture of Dulbecco's modified Eagle's medium and F12 nutrient (1:1 v/v) supplemented with 10% B27 (Gibco-BRL), 5% glutamine, and 1% penicillin-streptomycin-nystatin. After 24 h, the medium of the primary culture of neurons and astrocytes medium was replaced with a fresh one.

$A\beta_{42}$ preparation

Amyloid-beta (1–42) oligomers, $A\beta_{42}$, were prepared according to Amir et al. [2]. Briefly, $A\beta_{42}$ (3 mg) was dissolved in 10 mM NaOH, sonicated for 3 min, and then freeze-dried. The freeze-dried peptide was dissolved in 1 mM PBS. The mixture was split, the pH of the samples was adjusted to 7.4, and the samples were left at RT for 30 min to form oligomers. To evaluate the formation of oligomers, we measured the size of $A\beta_{42}$ aggregates by dynamic light scattering (DLS) and TEM. A primary culture of neurons and astrocytes was treated with 50 μM $A\beta_{42}$ in the presence or absence of SAS for 48 h. After 48 h the cells were tested for viability by dyeing them with trypan blue, and counting the vital cells.

Lactate Dehydrogenase (LDH) test

LDH activity was determined as previously described [21]. Briefly, 25 μL of the incubation media from the trypan blue assay were transferred into a 96-well plate, and the LDH activity was determined with an LDH-L kit (Thermo Electron, Melbourne, Australia). The product of the enzyme (formazan) was measured spectrophotometrically (Spectrafluor plus, Tecan, Switzerland) at 30°C at 340 nm.

Platelet aggregation testing

Blood from healthy donors, who had not been medicated for at least 15 days, was mixed with 3.8% sodium citrate (1:9 citrate/blood) incubated with SAS at different concentrations (0.2, 0.4, 1, 5, 25, 100, and 500 μM), and centrifuged (500 g for 15 min) to obtain platelet-poor plasma. Platelet-poor plasma was subjected to standard coagulation testing (prothrombin time, partial thromboplastin time, and Fibrinogen) with the coagulation analyzer ACL TOP 500 CTS (Instrumentation Laboratory).

Citrated blood from healthy donors was centrifuged (90 g for 15 min) to obtain platelet-rich plasma (PRP) for platelet aggregation testing, that was performed using a multi-channel Platelet Aggregation Profiler® model PAP-8E S/W Version 1.0.8 aggregometer (Bio/Data Corp.) Briefly, 225 μl of PRP suspension was maintained at 37°C in a siliconized glass cuvette and preincubated for 10 min with SAS at concentrations of 0, 0.02, 0.04, 0.2, 0.4, 1, 5, 25, 100, and 500 μM. Aggregation was initiated by adding 20 mM of ADP (MoLAB. Germany) and followed with constant stirring at 900 rpm for 12 min.

Animals

We used 5XFAD transgenic mice previously described by Oakley et al. [16]. Hemizygous transgenic mice were crossed with C57Bl/6J breeders. Genotyping was performed by PCR analysis of tail DNA. Littermates negative for the APP and PS1 transgenes were utilized as wild-type (WT) mice (female, $n = 8$; male, $n = 8$). 5XFAD mice of both sexes were randomly assigned to two groups, untreated mice (5XFAD) (female, $n = 6$; male, $n = 8$)

and SAS-treated mice (5XFAD+SAS) (female, $n = 7$; male, $n = 9$). The mice were kept in a 12-h light/dark cycle and had access to food and water ad libitum. Treatment started at the age of 2 months, and SAS (1 mg/kg dissolved in saline) was injected intraperitoneally (100 μl of solution) every day for two months. We initiated treatment at 2 months of age because amyloid deposition and related gliosis starts at 2 months in the 5XFAD mouse model [16]. Behavioral tests were conducted at the age of 6 months. We decided to evaluate the behavioral outcomes at 6 months of age since several studies demonstrated that at this age 5XFAD mice exhibit deficits in contextual and spatial memory as well as anxiety related behavior [16–19]. All animal experiments and protocols were approved by the Committee for Animal Research at Tel Aviv University.

Behavioral tests

Elevated plus maze

The elevated plus maze consisted of two anxiety-provoking open (without partitions) arms and two enclosed (with partitions) arms elevated 80 cm above the ground. Mice were placed at the junction between the open and enclosed arms of the plus maze and allowed to explore for 5 min. The maze was cleaned with 70% alcohol after testing of each mouse. Time spent in both open and closed arms was measured using the EthoVision XT 9 software platform (Noldus, Wageningen, Netherlands).

Y maze spontaneous alternation test

The Y maze comprised of three white plastic arms at a 120° angle from each other. Each mouse was situated at the center of the maze and allowed to freely explore the three arms. The number and the sequence of arms entered were recorded. Percentage of alternation was calculated as the number of alternations (entries into three different arms consecutively) divided by the total possible alternations (i.e., the number of arms entered minus 2) and multiplied by 100 [22].

Water T maze

The Water T maze assay was adapted from Guariglia et al. [23] The T maze apparatus consists of three opaque plexiglas arms. Each arm of the T maze was 18.5 cm long, 5 cm wide and 30 cm tall. The pool was filled with 23°C (±1°C) water to a depth of 13 cm, which was 1 cm above the surface of the platform. Mice were trained to swim to a particular arm of the T and to remain on a submerged platform for 5 s. Mice had to complete eight out of ten trials without error for two consecutive days to reach the learning criterion.

Immunohistochemistry and plaque quantification

At the end of the experiment, 3 female 5XFAD mice and 3 female SAS-treated 5XFAD mice were transcardially perfused, under ketamine/xylazine anesthesia, with cold saline, followed by paraformaldehyde 4% in phosphate buffer. The brains were immersed in 4% paraformaldehyde for 24 h at 4°C followed by cryoprotection in 30% sucrose for an additional 48 h. The brains were frozen in chilled 2-methylbutane (Sigma-Aldrich) and later sectioned into slices measuring 10 μm at –20°C.

Slides were treated with thioflavin S (Sigma-Aldrich T-1892), solved in sterile 50% ethanol to make a solution of 0.01% (w/V) and filtered before further dilution, as previously described [24]. Briefly, slides were incubated for 8 min in thioflavin S, washed for 10 min in 80% ethanol and then 10 min in H_2O, and subsequently stained with DAPI (0.05 mg/ml). For microscopic analysis, Axio Imager.Z2 microscope (Zeiss, Thornwood, NY) was used. Number of plaques was quantified in five serial coronal sections 250 μm apart in the hippocampus. %TioS area was calculated as number of stained plaques per hippocampal area.

Statistics

All data are expressed as the mean+SEM. Statistical analyses were performed using a commercial software (GraphPad Prism 7). Comparison between two groups were conducted using two-tailed *t*-test or one-tailed *t*-test (solely for the histological analysis). Comparisons between more than two treatment groups were conducted using either one-way analysis of variance (ANOVA) or two-way repeated measures ANOVA, followed by Tukey's *post-hoc* test. Statistical significance was considered for $p < 0.05$ in all statistical analyses.

RESULTS

SAS inhibits the formation and dissolves $A\beta_{42}$-Zn(II)/Cu(II) aggregates

Both Cu(II) and Zn(II) are released from vesicles of neurons during synaptic transmission, reaching concentrations as high as 15 μM [25] and 300 μM [26],

respectively. This homeostasis is disrupted in AD and the concentrations of Cu(II) and Zn(II) can rise up to ~1 mM [27, 28], and consequently promote Aβ aggregation [1, 29, 30].

Aggregation of Aβ-metal ion complexes results in a turbid solution, which affects the light scattering of the sample. The difference in the solution's turbidity is determined by the absorbance at 405 nm (A_{405nm}) [31], which indicates the degree of Aβ-Cu(II)/Zn(II) aggregation [31, 32].

Here, we measured the potential of SAS to inhibit the aggregation of $A\beta_{42}$-Zn(II)/ Cu(II) in amyloid beta and M(II)-ion solutions. In addition, we studied the ability of SAS to disassemble $A\beta_{42}$-Zn(II)/Cu(II) aggregates by adding SAS 1 h after mixing $A\beta_{42}$ with Zn(II)/Cu(II). We compared the activity of SAS to that of EDTA, a known metal chelator. We revealed that 150 μM SAS inhibited the formation of $A\beta_{42}$-Zn(II) aggregates by 60% and dissolved pre-formed $A\beta_{42}$-Zn(II) aggregates by 40% (Fig. 2A). In comparison, EDTA inhibited the formation of $A\beta_{42}$-Zn(II) aggregates only by 35% and dissolved $A\beta_{42}$-Zn(II) aggregates by 30% (Fig. 2A).

A similar result was obtained for $A\beta_{42}$-Cu(II) aggregates. 150 μM SAS inhibited the formation of $A\beta_{42}$-Cu(II) aggregates by 57%, and dissolved $A\beta_{42}$-Cu(II) aggregates by 40% (Fig. 2B). In this case, 150 μM EDTA was found to be more effective than SAS for the inhibition of the formation and disaggregation of $A\beta_{42}$-Cu(II) aggregates (89% inhibition and 80% disaggregation). We also measured the potential of SAS to inhibit the aggregation of $A\beta_{42}$ alone with no M(II)-ion by UV measurements and ThT assay, but no significant inhibition of the $A\beta_{42}$ aggregation was obtained (data not shown).

SAS rescues primary culture of neurons and astrocytes from $A\beta_{42}$ toxicity

Iron chelators have been shown to protect neuronal cells against the pro-apoptotic signaling of Aβ [33]. In order to study the neuroprotective activity of SAS, we exposed a primary culture of rat neurons and astrocytes to 50 μM $A\beta_{42}$ for 48 h with increasing doses of SAS. We demonstrated that treatment with 5 μM SAS resulted in survival of almost 80% of the cells, $IC_{50} = 0.5$ μM (Fig. 3A) (1-way ANOVA, $F_{6,33} = 60.2$, $p < 0.0001$; Tukey's multiple comparison test, for 50 μM $A\beta_{42}$ versus 5 μM SAS, $p = 0.0001$).

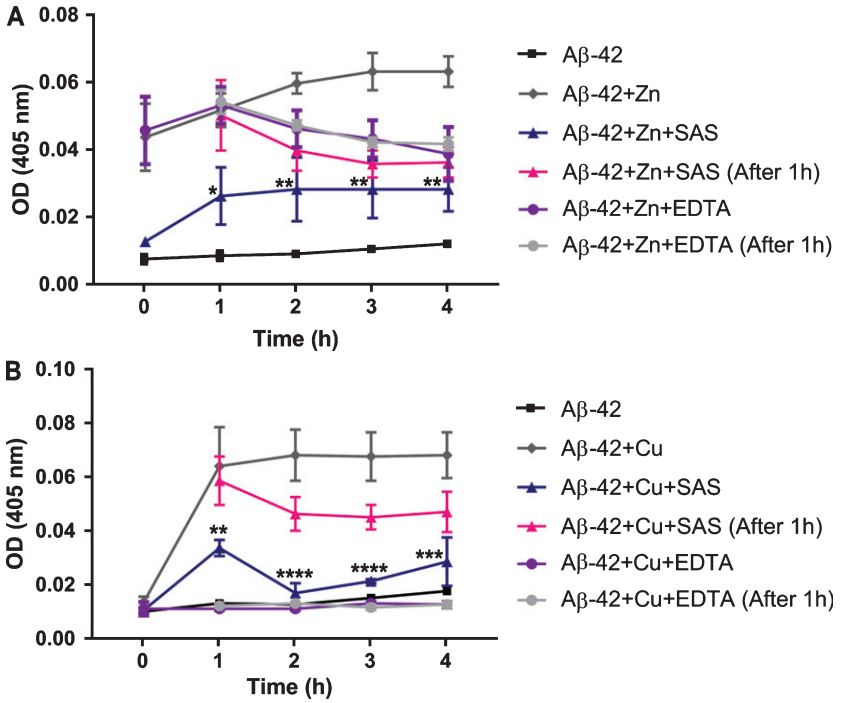

Fig. 2. Decomposition of (A) $A\beta_{42}$-Zn(II) or (B) $A\beta_{42}$-Cu(II) aggregates by SAS as compared to EDTA. The assay mixtures (tested compounds and $A\beta_{42}$-M(II) aggregates) were: 1) 50 μM $A\beta_{42}$; 2) 50 μM $A\beta_{42}$-Zn(II)/Cu(II); 3) 50 μM $A\beta_{42}$-Zn(II) + 150 μM SAS/EDTA; 4) 150 μM SAS or EDTA were added to ($A\beta_{42}$-Zn(II)/ Cu(II)) after 1 h. The samples were measured at 405 nm, every hour during 4 h of incubation. The results shown are the mean ± SEM of three independent experiments performed in duplicate. $^{*}p < 0.05$, $^{**}p < 0.01$, $^{***}p < 0.001$, $^{***}p < 0.0001$ versus $A\beta_{42}$+Zn/ $A\beta_{42}$+Cu treatment.

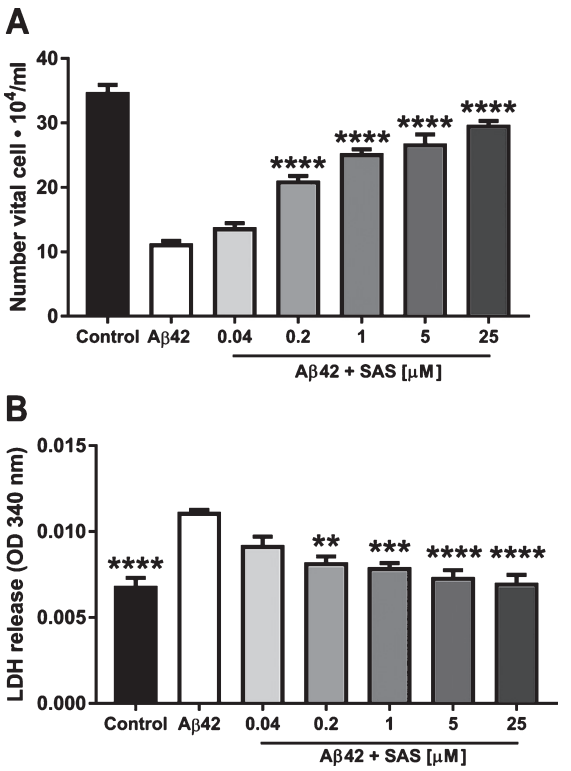

Fig. 3. Rescue of neurons from $A\beta_{42}$ toxicity by SAS. A) Primary neuronal cells were cultured in 96-well plates. The cells were treated with 50 μM $A\beta_{42}$ and 0.04–25 μM of SAS for 48 h. Cell viability was measured by dyeing the cells with trypan blue and counting the vital cells. The results shown are representative of three independent experiments performed in triplicate. B) The media of primary neuronal cells subjected to $A\beta_{42}$, was tested for LDH level. Samples from this media was transferred into a 96-well plate together with 100 μL of LDH testing reagent. The amount of LDH released to the extracellular fluid was measured spectrophotometrically at 30°C at 340 nm. $^{**}p<0.01$, $^{***}p<0.001$, $^{****}p<0.0001$ versus $A\beta_{42}$ treatment.

LDH levels, which elevate upon cell death, were measured in the culture media of the aforementioned experiment. Following treatment with 50 μM of $A\beta_{42}$, LDH level was elevated by 50% as compared to the control (1-way ANOVA, $F_{6,20}=9.835$, $P<0.0001$; Tukey's multiple comparison test, for 50 μM $A\beta_{42}$ versus control, $p=0.0001$). Treatment with SAS at 1 μM reduced the level of LDH to the basal level (Fig. 3B) (Tukey's multiple comparison test, for 50 μM $A\beta_{42}$ versus SAS at 1 μM, $p=0.0002$).

SAS does not cause platelet aggregation in human blood

Previously we found that SAS is a highly potent $P2Y_1R$ agonist (EC_{50} 2.6 nM). Furthermore, we have shown that co-application of SAS and antagonists of $P2Y_{12}R$ and $P2Y_1R$, reduced SAS neuroprotective effect in primary neurons exposed to oxidative stress [15]. Since $P2Y_1R$ and $P2Y_{12}R$ are involved in the process of platelet aggregation [34], we measured platelet aggregation following SAS treatment in whole human blood versus saline and Clopidogrel (a drug that inhibits $P2Y_{12}R$) controls.

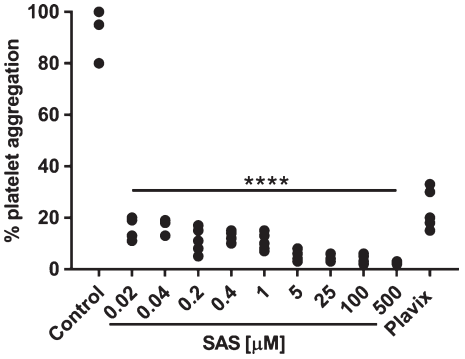

Fig. 4. Summary of aggregation results of platelets activated by ADP with different concentrations of SAS. Results represent at least 3–5 different subjects tested separately. Control: No drug; Plavix: Clopidogrel at therapeutic range. $^{****}p<0.0001$.

We revealed that platelet aggregation in response to ADP was significantly decreased with all concentrations of SAS tested. Aggregation inhibition was compared to values seen in patients taking Clopidogrel at doses of 75–100 mg/day, and was found to be very effective even at a low dose of 0.02 μM (Fig. 4, $F(10, 35)=120$, $p<0.0001$).

These results suggest differential effect of SAS on $P2Y_1R$ in neurons and platelets, with an agonist effect on neurons but antagonist effect on platelets. Thus, SAS acts as a potent anti-human platelet agent comparable to Clopidogrel at therapeutic doses.

In addition, we found that SAS at all tested concentrations (0.2–500 μM) did not significantly affect prothrombin time, activated partial thromboplastin time, and fibrinogen concentration, suggesting SAS does not affect blood coagulation. Moreover, no hemolytic effect of SAS was detected in whole human blood (data not shown).

SAS treatment prevented behavioral disinhibition in 5XFAD mice

We studied the therapeutic potential of SAS on cognitive and behavioral deficits in 6-months old 5XFAD mice, following two months of SAS treatment (1 mg/Kg/day) initiated at the age of 2 months. First, we utilized the elevated plus maze to exam-

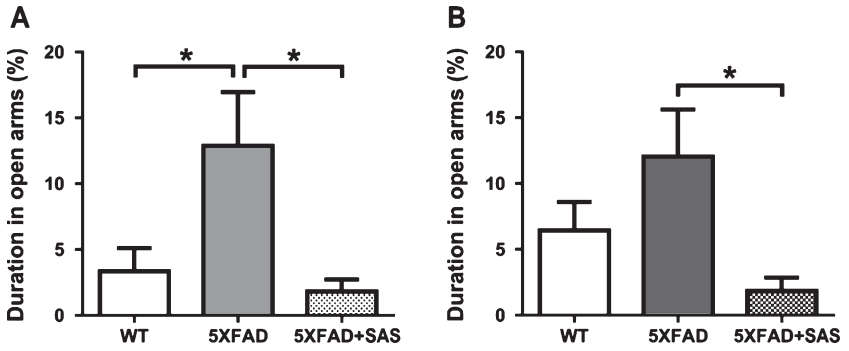

Fig. 5. SAS treatment prevents behavioral disinhibition of 5XFAD mice in the elevated plus maze. A, B) Percentages of duration of time spent in open arms versus total (open and closed arms). A) Female mice: WT, $n=8$; 5XFAD, $n=6$; 5XFAD+SAS, $n=7$. B) Male mice: WT, $n=8$, 5XFAD, $n=8$; 5XFAD+SAS, male, $n=9$. Error bars represent SEM. $^*p<0.05$. WT: wild-type; 5XFAD: untreated 5XFAD mice; 5XFAD+SAS: SAS-treated 5XFAD mice.

ine behavioral disinhibition previously observed in male [19] and female [35] 5XFAD mice. In order to assess motor function and exploratory activity we measured the number of arms entered during the test. 5XFAD mice (female and male) did not significantly differ in the number of arms visited during the test compared to wild-type (WT) control mice and SAS–treated 5XFAD mice (Female: 1-way ANOVA, $F_{2,18}=1.673$, $p=0.2156$; Male: 1-way ANOVA, $F_{2,22}=0.02965$, $p=0.9708$, data not shown). Female 5XFAD mice spent significantly more time exploring the anxiety-provoking open arms compared to wild-type (WT) control mice, indicating decreased anxiety, or behavioral disinhibition (Fig. 5A) (1-way ANOVA, $F_{2,18}=5.814$, $p=0.0113$; Tukey's multiple comparison test, for WT versus 5XFAD, $p=0.0296$). Similarly, male 5XFAD mice explored the anxiety-provoking open arms for a longer duration compared to WT mice, however, this result did not reach statistical significance (Fig. 5B) (1-way ANOVA, $F_{2,21}=4.279$, $p=0.0276$; Tukey's multiple comparison test for WT versus 5XFAD, $p=0.2646$). SAS-treated 5XFAD mice (female and male) spent significantly less time exploring the anxiety-provoking open arms, indicating intact performance in the elevated plus maze following SAS treatment (Fig. 5A, B) (Female: Tukey's multiple comparison test for 5XFAD versus 5XFAD+SAS, $p=0.0141$; Male: Tukey's multiple comparison test for 5XFAD versus 5XFAD+SAS, $p=0.0214$).

SAS treatment prevented spatial working memory deficit in 5XFAD mice

The Y-maze spontaneous alternation test is a common test for examining hippocampus-dependent spatial working memory in mice [22, 36]. 5XFAD mice (female and male) did not significantly differ in the number of arms visited compared to WT mice and SAS–treated 5XFAD mice (Female: 1-way ANOVA, $F_{2,18}=2.075$, $p=0.1546$; Male: 1-way ANOVA, $F_{2,22}=2.306$, $p=0.1232$, data not shown), indicating normal motor function and exploratory activity. Female 5XFAD mice did not show a decrease in alternation behavior compared to WT mice (Fig. 6A) (1-way ANOVA: $F_{2,18}=2.423$, $p=0.117$; Tukey's multiple comparison test, for WT versus 5XFAD, $p=0.3249$). Nevertheless, male 5XFAD mice demonstrated a significant decrease in alternation behavior compared to WT mice, indicating impaired spatial working memory. Importantly, SAS treatment prevented loss of normal alternation behavior in male 5XFAD mice (Fig. 6B) (1-way ANOVA: $F_{2,22}=4.999$, $p=0.0162$; Tukey's multiple comparison test, for WT versus 5XFAD, $p=0.021$; for 5XFAD versus 5XFAD+SAS, $p=0.0463$).

Interestingly, female 5XFAD mice took significantly more training days to reach the learning criterion compared to WT mice (Fig. 6C) (1-way ANOVA: $F_{2,18}=3.978$, $p=0.0371$; Tukey's multiple comparison test, for WT versus 5XFAD, $p=0.0458$). SAS treatment decreased the number of training days it took female 5XFAD mice to reach the learning criterion (2.7d versus 4d), though this result did not reach statistical significance but a strong trend toward significance (Fig. 6C) (Tukey's multiple comparison test for 5XFAD versus 5XFAD+SAS, $p=0.0731$). In contrast, male 5XFAD mice did not exhibit a significant increase in the number of training days required to reach the learning criterion compared to WT mice (Fig. 6D) (1-way ANOVA: $F_{2,22}=0.9855$,

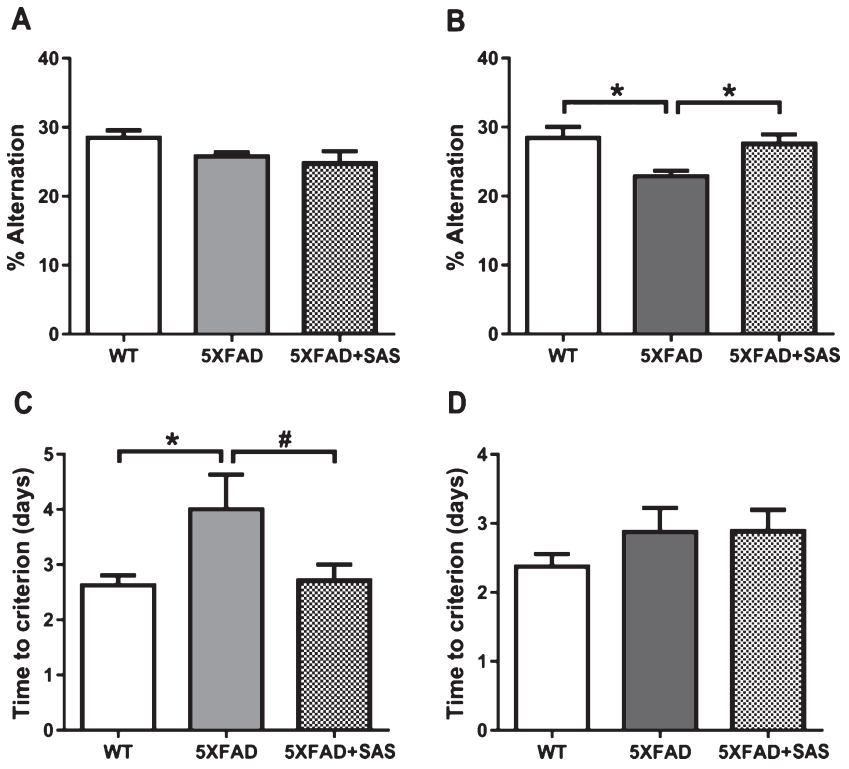

Fig. 6. SAS treatment ameliorates spatial working memory deficits. A, B) Percentage of alternation is calculated as number of triads including entries into all three arms/maximum possible alternations (total number of arms entered –2)*100. C, D) Number of training days required to reach the learning criterion. A,C) Female mice: WT, $n=8$; 5XFAD, $n=6$; 5XFAD+SAS, $n=7$. B,D) Male mice: WT, $n=8$, 5XFAD, $n=8$; 5XFAD+SAS, male, $n=9$. Error bars represent SEM. $^{*}p<0.05$. $^{\#}p=0.0731$. WT, wild-type; 5XFAD, untreated 5XFAD mice; 5XFAD+SAS, SAS-treated 5XFAD mice.

$p=0.3891$; Tukey's multiple comparison test, for WT versus 5XFAD, $p=0.4736$).

Effect of SAS treatment on amyloid plaques

At the end of the behavioral assesment, 3 female 5XFAD mice and 3 female SAS-treated 5XFAD mice (6 months old) were sacrificed and their brains were taken for tissue analysis as an evaluation of the effect of SAS on amyloid plaque burden. We quantified amyloid deposition using thioflavin S staining in the hippocampus. SAS-treated 5XFAD mice showed a very strong trend toward a decrease in the number of thioflavin S-positive amyloid plaques (Supplementary Figure 1) ($t_4=2.128$, $p=0.0502$).

DISCUSSION

The main features of AD include amyloid plaques, neurofibrillary tangles [37], oxidative stress [38], and neuroinflammatory processes [39]. Previously, we found that nucleoside 5′-phosphorothioate analogues, ATP-γ-S and especially ADP-β-S, effectively dissolved $A\beta_{40}$-Cu(I) and $A\beta_{42}$-Cu(II)/Zn(II) aggregates [2]. Recently, we found that nucleoside 5′-phosphorothioate analogue SAS, reduced ROS production in PC12 cells under oxidizing conditions, rescued primary neurons subjected to $FeSO_4$ oxidation and helped maintain the normal morphology of the neurons undergoing oxidative insult [15]. The ion chelating properties of SAS encouraged us to apply it for targeting an AD pathological feature, namely, metal-ion induced-Aβ aggregation. $A\beta_{42}$ and $A\beta_{40}$ are the most common forms of Aβ in brains of AD patients [40]. However, $A\beta_{42}$ has a higher tendency to aggregate than $A\beta_{40}$ due to its two hydrophobic terminal residues, and was found to be more toxic to neuron cells [41–43]. The aggregation of $A\beta_{40/42}$ is further accelerated by Cu(II) and Zn(II) [1, 2, 29, 30].

Here, we used the rapidly precipitating $A\beta_{42}$-Cu(II)/Zn(II) aggregates to assess the ability of SAS to inhibit and dissolve Aβ-metal-ion aggregates. We found that 150 μM SAS inhibited the formation of

$A\beta_{42}$-Zn(II) aggregates 2-fold more efficiently than EDTA and was more efficient for dissolution of these aggregates. However, EDTA was more effective for inhibiting the formation of $A\beta_{42}$-Cu(II) and for dissolving these aggregates than SAS. Indeed, EDTA binds Cu(II) ions 200-fold stronger than Zn(II) ions ($K = 6.3 \cdot 10^{18}$ and $3.1 \cdot 10^{16}$, respectively) [44, 45]. Although SAS did not inhibit the aggregation of $A\beta_{42}$ alone (with no M(II) ions), the inhibition effect in the presence of M(II) ions is more relevant and probably mimics the pathological feature.

Encouraged by these data, we explored whether SAS can rescue neurons from $A\beta_{42}$-induced cell death, using primary mixed culture of rat astrocytes and neurons. By measuring the percentage of vital cells and LDH levels, we showed that SAS markedly improved the cell viability of this culture.

Our previously reported results suggest that in addition to its antioxidant activity (i.e., inhibition of Fenton reaction), SAS also activates $P2Y_1$-R and $P2Y_{12}$-R [15]. Earlier studies showed that ATP and $P2Y_1$ receptor agonist, 2-methylthio-ADP, protect cultured astrocytes against H_2O_2 toxicity, by activation of $P2Y_1$ receptors. It was suggested that activation of $P2Y_1$ receptors coupled to Gq/11 upregulates oxidoreductase genes [46].

P2Y receptor activation *in vitro* is reported to be protective by antioxidant and antiapoptotic actions. However, *in vivo* studies showed that P2Y receptor blocking in models of brain damage resulted in improved outcome. The contradictory evidence regarding the role of P2Y receptors in neuropathological conditions was recently thoroughly reviewed [47]. As opposed to cellular models, animal models involve interactions between different cell types, including neurons, astrocytes and microglia which contribute to the pathogenesis of neurodegenerative diseases. Using selective antagonists, we have shown that the neuroprotectant activity of SAS involves activation of both $P2Y_1$-R and $P2Y_{12}$-R in primary mixed culture of rat astrocytes and neurons [15]. The role of *in vivo* purinergic receptors activation by SAS, within brains of 5XFAD mice, warrants further exploration in future studies.

Importantly, in addition to the role of $P2Y_1$ and $P2Y_{12}$-R in neuroprotection, they also play a role in blood coagulation. Studies using selective $P2Y_1$-R antagonists confirmed its involvement in adenine-nucleotide induced platelet shape change and aggregation [48]. Likewise, the physiological role of $P2Y_{12}$ receptor in aggregation response to ADP is well established [49, 50]. These findings raised the question whether SAS may have adverse effects on blood coagulation. Hence, we evaluated the effect of SAS on human blood. We found that not only did SAS not induce platelet aggregation up to 500 μM but rather effectively inhibited platelet aggregation in response to ADP (the natural agonist of $P2Y_{1/12}$-R). Thus, the question of the lack of $P2Y_{1/12}$-R agonist activity of SAS in blood platelets remains open. We speculate that it may be related to the ability of P2Y receptors to form homo- or heterooligomers with each other or interact with other receptors in neurons and glia cells [47], thus resulting in different pharmacological effect in blood compared to the brain.

To further explore the therapeutic potential of SAS in AD, we used the widely-accepted AD mouse model, 5XFAD, that demonstrates behavioral and cognitive deficits. We showed that administration of a low dose of SAS (1 mg/Kg/day) for two months, initiated at the age of two months, prevented behavioral disinhibition and deficits in spatial working memory in 6-month-old 5XFAD mice.

Previous studies have shown that both female [35] and male [19] 5XFAD mice exhibit behavioral disinhibition in the elevated plus maze paradigm. Indeed, in our study both sexes demonstrated behavioral disinhibition indicated by spending longer time in the anxiety-provoking open arms. Remarkably, SAS treatment completely prevented the emergence of this defected phenotype in both female and male 5XFAD mice.

The most commonly used paradigms for working memory in rodents are maze tasks which require spatial working memory to navigate properly. The earliest variants of these are the Y-maze and T-maze alternation tasks, which are rather simple tests consisting of three arms with a single intersection. These tasks rely on the natural exploratory behavior of rodents and exploit the inherent tendency of animals to choose an alternative arm over an arm that has been previously explored on consecutive trials [51].

Previous studies reported impaired alternation performance in the Y-maze in 5XFAD mice as early as 4-5 months [16]. Here, we demonstrate that male, but not female, 5XFAD mice exhibit deficits in alternation performance in the Y-maze. Importantly, SAS treatment prevented the deficit in spatial working memory in these mice. In contrast, only female 5XFAD mice showed impaired alternation performance in the T-maze test. SAS treated 5XFAD female mice exhibited markedly improved spatial working memory in the T maze alternation test. Similar to our

work, previous studies have shown sex differences in terms of behavioral and biochemical changes in 5XFAD mice [52–54]. For example, Devi et al. [53] revealed that amyloid plaque formation was accelerated specifically in the female 5XFAD hippocampus following 5-day exposure to restraint stress. This finding may explain, at least in part, sex-specific cognitive deficits found in our study, as only female 5XFAD mice showed impaired performance in the "wet" T-maze task which is a relatively stressful test that involves swimming compared to the "dry" Y maze.

Deshpande et al. previously demonstrated that a local increase in the concentration of zinc as a result of synaptic activity may attract and facilitate aggregation of Aβ oligomers at the synaptic cleft [55]. Preclinical studies have shown that Clioquinol, an 8-OH quinoline with moderate affinity for zinc and copper, inhibits metal-induced Aβ aggregation in a transgenic mouse model of AD [56], and that PBT2, an 8-OH quinoline that lacks iodine, induced an improvement in learning and memory in transgenic models of AD [57]. Moreover, clinical studies provided encouraging data concerning the safety, efficacy and biomarkers findings of PBT2 in targeting Aβ as a therapeutic intervention for AD [58–60].

Notably, the 5XFAD mice were treated at the age of 2 months, before the onset of AD symptoms, for a duration of two months, while the effect was demonstrated in the age of 6 months. Thus, our results indicate that SAS has the potential to delay the progression of the cognitive decline and behavioural disinhibition which are core pathological characteristics of AD.

CONCLUSION

SAS, a biocompatible and water soluble small molecule, is highly effective in delaying pathological signs of AD, in a most aggressive animal model (5XFAD) at a low dose (1 mg/Kg/day). This compound showed no adverse effects in terms of platelets aggregation in human blood. Our findings here, in addition to our previous studies [15], imply that SAS acts via several mechanisms which include antioxidation (mainly by metal-ion chelation), inhibition of $A\beta_{42}$-M(II) aggregation and disassembly of aggregates, and possibly activation of purinergic receptors. Our data demonstrate the highly promising therapeutic effect of SAS in the 5XFAD mouse model. Additional studies on other AD models are warranted to strengthen the potential of this drug candidate.

DISCLOSURE STATEMENT

Authors' disclosures avaialble online (http://j-alz.com/manuscript-disclosures/16-1236r2).

SUPPLEMENTARY MATERIAL

The supplementary material is available in the electronic version of this article: http://dx.doi.org/10.3233/JAD-161236.

REFERENCES

[1] Faller P, Hureau C (2009) Bioinorganic chemistry of copper and zinc ions coordinated to amyloid-β peptide. *Dalton Trans* **298**, 1080-1094.

[2] Amir A, Shmuel E, Zagalsky R, Sayer AH, Nadel Y, Fischer B (2012) Nucleoside-5'-phosphorothioate analogues are biocompatible antioxidants dissolving efficiently amyloid beta-metal ion aggregates. *Dalton Trans* **41**, 8539-8549.

[3] Adlard PA, Bush AI (2006) Metals and Alzheimer's disease. *J Alzheimers Dis* **10**, 145-163.

[4] Yuan Y, Niu F, Liu Y, Lu N (2014) Zinc and its effects on oxidative stress in Alzheimer's disease. *Neurol Sci* **35**, 923-928.

[5] Eskici G, Axelsen PH (2012) Copper and oxidative stress in the pathogenesis of Alzheimer's disease. *Biochemistry* **51**, 6289-6311.

[6] Bush AI, Tanzi RE (2008) Therapeutics for Alzheimer's disease based on the metal hypothesis. *Neurotherapeutics* **5**, 421-432.

[7] Danino O, Grossman S, Fischer B (2015) ATP-γ-S-(α,β-CH2) protects against oxidative stress and amyloid beta toxicity in neuronal culture. *Biochem Biophys Res Commun* **460**, 446-450.

[8] Jacobson KA, Boeynaems JM (2010) P2Y nucleotide receptors: Promise of therapeutic applications. *Drug Discov Today* **15**, 570-578.

[9] Abbracchio MP, Burnstock G, Verkhratsky A, Zimmermann H (2009) Purinergic signalling in the nervous system: An overview. *Trends Neurosci* **32**, 19-29.

[10] Volonté C, Amadio S, Cavaliere F, D'Ambrosi N, Vacca F, Bernardi G (2003) Extracellular ATP and neurodegeneration. *Curr Drug Targets CNS Neurol Disord* **2**, 403-412.

[11] Schwiebert EM (2003) *Extracellular nucleotides and nucleosides: Release, receptors, and physiological and pathophysiological effects,* Academic Press.

[12] Fields RD, Burnstock G (2006) Purinergic signalling in neuron–glia interactions. *Nat Rev Neurosci* **7**, 423-436.

[13] Tonazzini I, Trincavelli ML, Storm-Mathisen J, Martini C, Bergersen LH (2007) Co-localization and functional cross-talk between A1 and P2Y1 purine receptors in rat hippocampus. *Eur J Neurosci* **26**, 890-902.

[14] Zheng W, Talley Watts L, Holstein DM, Wewer J, Lechleiter JD (2013) P2Y1R-initiated, IP3R-dependent stimulation of astrocyte mitochondrial metabolism reduces and partially reverses ischemic neuronal damage in mouse. *J Cereb Blood Flow Metab* **33**, 600-611.

[15] Azran S, Danino O, Förster D, Kenigsberg S, Reiser G, Dixit M, Singh V, Major DT, Fischer B (2015) Identification of highly promising antioxidants/neuroprotectants

based on nucleoside 5′-phosphorothioate scaffold. Synthesis, activity, and mechanisms of action. *J Med Chem* **58**, 8427-8443.

[16] Oakley H, Cole SL, Logan S, Maus E, Shao P, Craft J, Guillozet-Bongaarts A, Ohno M, Disterhoft J, Van Eldik L, Berry R, Vassar R (2006) Intraneuronal beta-amyloid aggregates, neurodegeneration, and neuron loss in transgenic mice with five familial Alzheimer's disease mutations: Potential factors in amyloid plaque formation. *J Neurosci* **26**, 10129-10140.

[17] Kimura R, Ohno M (2009) Impairments in remote memory stabilization precede hippocampal synaptic and cognitive failures in 5XFAD Alzheimer mouse model. *Neurobiol Dis* **33**, 229-235.

[18] Ohno M, Chang L, Tseng W, Oakley H, Citron M, Klein WL, Vassar R, Disterhoft JF (2006) Temporal memory deficits in Alzheimer's mouse models: Rescue by genetic deletion of BACE1. *Eur J Neurosci* **23**, 251-260.

[19] Schneider F, Baldauf K, Wetzel W, Reymann KG (2014) Behavioral and EEG changes in male 5xFAD mice. *Physiol Behav* **135**, 25-33.

[20] Danino O, Giladi N, Grossman S, Fischer B (2014) Nucleoside 5′-phosphorothioate derivatives are highly effective neuroprotectants. *Biochem Pharmacol* **88**, 384-392.

[21] Shneyvays V, Safran N, Halili-Rutman I, Shainberg A (2000) Insights into adenosine A1 and A3 receptors function: Cardiotoxicity and cardioprotection. *Drug Dev Res* **50**, 324-337.

[22] Sarnyai Z, Sibille EL, Pavlides C, Fenster RJ, McEwen BS, Toth M (2000) Impaired hippocampal-dependent learning and functional abnormalities in the hippocampus in mice lacking serotonin 1A receptors. *Proc Natl Acad Sci U S A* **97**, 14731-14736.

[23] Guariglia SR, Chadman KK (2013) Water T-maze: A useful assay for determination of repetitive behaviors in mice. *J Neurosci Methods* **220**, 24-29.

[24] Glat M, Skaat H, Menkes-Caspi N, Margel S, Stern EA (2013) Age-dependent effects of microglial inhibition *in vivo* on Alzheimer's disease neuropathology using bioactive-conjugated iron oxide nanoparticles. *J Nanobiotechnology* **11**, 32.

[25] Hartter DE, Barnea A (1988) Evidence for release of copper in the brain: Depolarization-induced release of newly taken-up 67copper. *Synapse* **2**, 412-415.

[26] Frederickson CJ (1989) Neurobiology of zinc and zinc-containing neurons. *Int Rev Neurobiol* **31**, 145-238.

[27] Bush AI (2003) The metallobiology of Alzheimer's disease. *Trends Neurosci* **26**, 207-214.

[28] Dedeoglu A, Cormier K, Payton S, Tseitlin KA, Kremsky JN, Lai L, Li X, Moir RD, Tanzi RE, Bush AI, Kowall NW, Rogers JT, Huang X (2004) Preliminary studies of a novel bifunctional metal chelator targeting Alzheimer's amyloidogenesis. *Exp Gerontol* **39**, 1641-1649.

[29] Lovell M, Robertson J, Teesdale W, Campbell J, Markesbery W (1998) Copper, iron and zinc in Alzheimer's disease senile plaques. *J Neurol Sci* **158**, 47-52.

[30] Tõugu V, Palumaa P (2012) Coordination of zinc ions to the key proteins of neurodegenerative diseases: Aβ, APP, α-synuclein and PrP. *Coord Chem Rev* **256**, 2219-2224.

[31] Storr T, Scott LE, Bowen ML, Green DE, Thompson KH, Schugar HJ, Orvig C (2009) Glycosylated tetrahydrosalens as multifunctional molecules for Alzheimer's therapy. *Dalton Trans* **3**, 3034.

[32] Huang X, Atwood CS, Moir RD, Hartshorn MA, Vonsattel J-P, Tanzi RE, Bush AI (1997) Zinc-induced Alzheimer's Abeta 1-40 aggregation is mediated by conformational factors. *J Biol Chem* **272**, 26464-26470.

[33] Kuperstein F, Yavin E (2004) Pro-apoptotic signaling in neuronal cells following iron and amyloid beta peptide neurotoxicity. *J Neurochem* **86**, 114-125.

[34] Jin J, Kunapuli SP (1998) Coactivation of two different G protein-coupled receptors is essential for ADP-induced platelet aggregation. *Proc Natl Acad Sci U S A* **95**, 8070-8074.

[35] Wirths O, Erck C, Martens H, Harmeier A, Geumann C, Jawhar S, Kumar S, Multhaup G, Walter J, Ingelsson M, Degerman-Gunnarsson M, Kalimo H, Huitinga I, Lannfelt L, Bayer TA (2010) Identification of low molecular weight pyroglutamate Aβ oligomers in Alzheimer disease: A novel tool for therapy and diagnosis. *J Biol Chem* **285**, 41517-41524.

[36] Bryan KJ, Lee H, Perry G, Smith MA, Casadesus G (2009) Transgenic mouse models of Alzheimer's disease: Behavioral testing and considerations. In *Methods of Behavior Analysis in Neuroscience*, 2nd edition. Buccafusco JJ, ed. CRC Press/Taylor & Francis, Boca Raton, FL.

[37] Iqbal K, del C, Alonso A, Chen S, Chohan MO, El-Akkad E, Gong C-X, Khatoon S, Li B, Liu F, Rahman A, Tanimukai H, Grundke-Iqbal I (2005) Tau pathology in Alzheimer disease and other tauopathies. *Biochim Biophys Acta* **1739**, 198-210.

[38] Praticò D (2008) Oxidative stress hypothesis in Alzheimer's disease: A reappraisal. *Trends Pharmacol Sci* **29**, 609-615.

[39] Akiyama H, Barger S, Barnum S, Bradt B, Bauer J, Cole GM, Cooper NR, Eikelenboom P, Emmerling M, Fiebich BL, Finch CE, Frautschy S, Griffin WST, Hampel H, Hull M, Landreth G, Lue LF, Mrak R, MacKenzie IR, McGeer PL, O'Banion MK, Pachter J, Pasinetti G, Plata-Salaman C, Rogers J, Rydel R, Shen Y, Streit W, Strohmeyer R, Tooyoma I, Van Muiswinkel FL, Veerhuis R, Walker D, Webster S, Wegrzyniak B, Wenk G, Wyss-Coray T (2000) Inflammation and Alzheimer's disease. *Neurobiol Aging* **21**, 383-421.

[40] Mawuenyega KG, Sigurdson W, Ovod V, Munsell L, Kasten T, Morris JC, Yarasheski KE, Bateman RJ, Hardy J, Selkoe DJ, Cummings JL, Scheuner D, Bateman RJ, Bateman RJ, DeMattos RB, Ellis RJ (2010) Decreased clearance of CNS beta-amyloid in Alzheimer's disease. *Science* **330**, 1774.

[41] Jarrett JT, Berger EP, Lansbury PT (1993) The carboxy terminus of the beta. amyloid protein is critical for the seeding of amyloid formation: Implications for the pathogenesis of Alzheimer's disease. *Biochemistry* **32**, 4693-4697.

[42] Harper JD, Wong SS, Lieber CM, Lansbury PT (1997) Observation of metastable Aβ amyloid protofibrils by atomic force microscopy. *Chem Biol* **4**, 119-125.

[43] Hardy J, Selkoe DJ (2002) The amyloid hypothesis of Alzheimer's disease: Progress and problems on the road to therapeutics. *Science* **297**, 353-356.

[44] Martin RB (1994) Aluminum: A neurotoxic product of acid rain. *Acc Chem Res* **27**, 204-210.

[45] Smith RM, Martell AE, Motekaitis RJ (2004) "*NIST standard reference database 46." NIST Critically Selected Stability Constants of Metal Complexes Database Ver 2 (2004),* National Institute of Standards & Technology.

[46] Shinozaki Y, Koizumi S, Ishida S, Sawada J-I, Ohno Y, Inoue K (2005) Cytoprotection against oxidative stress-induced damage of astrocytes by extracellular ATP via P2Y1 receptors. *Glia* **49**, 288-300.

[47] Förster D, Reiser G (2015) Supportive or detrimental roles of P2Y receptors in brain pathology?-The two faces of P2Y receptors in stroke and neurodegeneration detected in

neural cell and in animal model studies. *Purinergic Signal* **11**, 441-454.

[48] Abbracchio MP, Burnstock G, Boeynaems J-M, Barnard EA, Boyer JL, Kennedy C, Knight GE, Fumagalli M, Gachet C, Jacobson KA, Weisman GA (2006) International Union of Pharmacology LVIII: Update on the P2Y G protein-coupled nucleotide receptors: From molecular mechanisms and pathophysiology to therapy. *Pharmacol Rev* **58**, 281-341.

[49] Gachet C (2006) Regulation of platelet functions by P2 receptors. *Annu Rev Pharmacol Toxicol* **46**, 277-300.

[50] Cattaneo M (2011) The platelet $P2Y^{12}$ receptor for adenosine diphosphate: Congenital and drug-induced defects. *Blood* **117**, 2102-2112.

[51] Dudchenko PA (2004) An overview of the tasks used to test working memory in rodents. *Neurosci Biobehav Rev* **28**, 699-709.

[52] Prange-Kiel J, Dudzinski DA, Pröls F, Glatzel M, Matschke J, Rune GM (2016) Aromatase Expression in the Hippocampus of AD Patients and 5xFAD Mice. *Neural Plast* **2016**, 1-11.

[53] Devi L, Alldred MJ, Ginsberg SD, Ohno M (2010) Sex- and brain region-specific acceleration of β-amyloidogenesis following behavioral stress in a mouse model of Alzheimer's disease. *Mol Brain* **3**, 34.

[54] Roddick KM, Schellinck HM, Brown RE (2014) Olfactory delayed matching to sample performance in mice: Sex differences in the 5XFAD mouse model of Alzheimer's disease. *Behav Brain Res* **270**, 165-170.

[55] Deshpande A, Kawai H, Metherate R, Glabe CG, Busciglio J (2009) A role for synaptic zinc in activity-dependent Abeta oligomer formation and accumulation at excitatory synapses. *J Neurosci* **29**, 4004-4015.

[56] Cherny RA, Atwood CS, Xilinas ME, Gray DN, Jones WD, McLean CA, Barnham KJ, Volitakis I, Fraser FW, Kim Y-S, Huang X, Goldstein LE, Moir RD, Lim JT, Beyreuther K, Zheng H, Tanzi RE, Masters CL, Bush AI (2001) Treatment with a copper-zinc chelator markedly and rapidly inhibits β-amyloid accumulation in Alzheimer's disease transgenic mice. *Neuron* **30**, 665-676.

[57] Adlard PA, Cherny RA, Finkelstein DI, Gautier E, Robb E, Cortes M, Volitakis I, Liu X, Smith JP, Perez K, Laughton K, Li Q-X, Charman SA, Nicolazzo JA, Wilkins S, Deleva K, Lynch T, Kok G, Ritchie CW, Tanzi RE, Cappai R, Masters CL, Barnham KJ, Bush AI (2008) Rapid restoration of cognition in Alzheimer's transgenic mice with 8-hydroxy quinoline analogs is associated with decreased interstitial Aβ. *Neuron* **59**, 43-55.

[58] Ritchie CW, Bush AI, Mackinnon A, Macfarlane S, Mastwyk M, MacGregor L, Kiers L, Cherny R, Li Q-X, Tammer A, Carrington D, Mavros C, Volitakis I, Xilinas M, Ames D, Davis S, Beyreuther K, Tanzi RE, Masters CL (2003) Metal-protein attenuation with iodochlorhydroxyquin (clioquinol) targeting Aβ amyloid deposition and toxicity in Alzheimer disease. *Arch Neurol* **60**, 1685.

[59] Lannfelt L, Blennow K, Zetterberg H, Batsman S, Ames D, Harrison J, Masters CL, Targum S, Bush AI, Murdoch R, Wilson J, Ritchie CW (2008) Safety, efficacy, and biomarker findings of PBT2 in targeting Aβ as a modifying therapy for Alzheimer's disease: A phase IIa, double-blind, randomised, placebo-controlled trial. *Lancet Neurol* **7**, 779-786.

[60] Faux NG, Ritchie CW, Gunn A, Rembach A, Tsatsanis A, Bedo J, Harrison J, Lannfelt L, Blennow K, Zetterberg H, Ingelsson M, Masters CL, Tanzi RE, Cummings JL, Herd CM, Bush AI (2010) PBT2 rapidly improves cognition in Alzheimer's disease: Additional phase II analyses. *J Alzheimers Dis* **20**, 509-516.